Systemic anti-VEGF treatment strongly reduces skin inflammation in a mouse model of psoriasis

Helia B. Schonthaler[a,b], Reto Huggenberger[c], Stefanie K. Wculek[a], Michael Detmar[c], and Erwin F. Wagner[a,1]

[a]Banco Bilbao Vizcaya Argentaria (BBVA)-Foundation, Cancer Cell Biology Programme, Centro Nacional de Investigaciones Oncológicas (CNIO), 28029 Madrid, Spain; [b]Research Institute of Molecular Pathology (IMP), Vienna, Austria; and [c]Institute of Pharmaceutical Sciences, Swiss Federal Institute of Technology, ETH Zurich, 8093 Zurich, Switzerland

Edited by Michael Karin, University of California, San Diego School of Medicine, La Jolla, CA, and approved October 22, 2009 (received for review July 8, 2009)

Although vascular remodeling is a hallmark of many chronic inflammatory disorders such as rheumatoid arthritis, inflammatory bowel disease, and psoriasis, anti-vascular strategies to treat these conditions have received little attention to date. We investigated the anti-inflammatory activity of systemic blockade of VEGF-A by the inhibitory monoclonal antibody G6–31, employing a therapeutic trial in a mouse model of psoriasis. Simultaneous deletion of *JunB* and *c-Jun* (DKO*) in the epidermis of adult mice leads to a psoriasis-like phenotype with hyper- and parakeratosis and increased subepidermal vascularization. Moreover, an inflammatory infiltrate and elevated levels of cytokines/chemokines including TNFα, IL-1α/β, IL-6, and the innate immune mediators IL-22, IL-23, IL-23R, and IL-12p40 are detected. Here we show that anti-VEGF antibody treatment of mice already displaying disease symptoms resulted in an overall improvement of the psoriatic lesions leading to a reduction in the number of blood vessels and a significant decrease in the size of dermal blood and lymphatic vessels. Importantly, anti-VEGF–treated mice showed a pronounced reduction of inflammatory cells within the dermis and a normalization of epidermal differentiation. These results demonstrate that systemic blockade of VEGF by an inhibitory antibody might be used to treat patients who have inflammatory skin disorders such as psoriasis.

activator protein-1 | Jun proteins | epidermis | angiogenesis | G6-31 antibody

Angiogenesis has an important role in tumor growth and metastasis. However, vascular remodeling also occurs in many inflammatory and autoimmune disorders (1, 2), including rheumatoid arthritis, inflammatory bowel disease, and the chronic inflammatory skin disease, psoriasis (3–5). Psoriasis affects ≈2% of the world population and is characterized by epidermal hyperplasia, inflammatory infiltrates, enlarged, tortuous, and hyperpermeable blood vessels, and an enlargement of lymphatic vessels (6, 7). Several studies indicate a crucial role of VEGF-A (here termed "VEGF") in the pathogenesis of psoriasis: (*i*) epidermis-derived VEGF is strongly up-regulated in psoriatic skin lesions (8); (*ii*) VEGF serum levels are correlated with disease severity (9); (*iii*) a genetic predisposition caused by single-nucleotide polymorphisms of the VEGF gene may be involved in the pathogenesis of psoriasis (10); and (*iv*) K14-VEGF transgenic mice expressing mouse VEGF164 in the epidermis spontaneously develop a chronic psoriasiform skin inflammation (6). Moreover, VEGF transgenic mice show the characteristic Koebner phenomenon, because induction of skin inflammation in transgenic mice results in the development of chronic, psoriasis-like skin inflammation (7). Treatment of K14-VEGF transgenic mice with a VEGF receptor tyrosine-kinase inhibitor, NVP-BAW288, reduced the number of blood and lymphatic vessels and the infiltrating leukocytes in the skin and normalized the epidermal architecture (11). Recently developed anti-psoriatic therapies (e.g., ustekinumab and ABT-874) predominantly target specific components of the immune system, such as TNFα, or molecules involved in T-cell activation (12–14); however, no cure is currently available (15). Surprisingly anti-angiogenic treatments for chronic inflammatory conditions have received little attention thus far, although some therapies for psoriasis, such as paclitaxel and shark fin cartilage, are thought to have an anti-angiogenic effect (16). Moreover, the prominent involvement of angiogenesis in the pathogenesis of psoriasis and the validated use of anti-angiogenic therapy in human cancers using a monoclonal antibody directed against VEGF (bevacizumab, Avastin^R) (17, 18) suggests anti-VEGF treatment as a possible therapy for patients suffering from psoriasis. Recently, a patient was reported to experience complete remission of psoriasis during bevacizumab treatment of metastatic colon cancer (19).

Jun proteins are members of the transcription factor complex AP-1 and are essential in establishing and maintaining skin homeostasis (20). Epidermal *c-Jun* controls keratinocyte proliferation and differentiation by regulating the expression of epidermal growth factor receptor and heparin-binding EGF-like growth factor (21). On the other hand, absence of epidermal *JunB* in mice leads to ulcerative skin lesions and a multiorgan disease caused by the secretion of granulocyte colony-stimulating factor and IL-6 by keratinocytes (22).

In the present study we used a therapeutic approach in a genetic mouse model of chronic, psoriasis-like skin inflammation (20, 23, 24), using the anti-VEGF antibody G6–31, which potently inhibits both human and murine VEGF (25). After Cre-mediated deletion, mice carrying floxed alleles for *JunB* and *c-Jun* develop a chronic, psoriasis-like skin inflammation comprising many immunological features observed in human psoriatic patients (23). Systemic treatment of mutant mice with an anti-VEGF antibody strongly reduced skin inflammation within 8 days of treatment in contrast with control IgG-treated animals. The mutant mice showed an overall improvement of the psoriatic phenotype, normalization of the epidermal architecture, and a reduction in the number and size of blood vessels. Moreover, the immune infiltrate in the skin was reduced in antibody-treated mice.

Results

Systemic Inhibition of VEGF Reduces the Psoriasis-Like Skin Inflammation. The effects of the monoclonal anti-VEGF antibody G6–31 (25) were tested in a mouse model displaying many characteristic features of psoriasis. Eight-week-old mice carrying floxed alleles for the *JunB* and *c-Jun* locus and the K5-CreER^T transgene received consecutive i.p. injections of tamoxifen (1 mg/day) for a period of 5 days. This treatment leads to the deletion of both genes in the epidermis by inducible Cre-recombinase activity (see also *SI Materials and Methods*). When the mice showed the first symptoms of a psoriatic phenotype (10–11 days after the last tamoxifen injec-

Author contributions: H.B.S., M.D., and E.F.W. designed research; H.B.S., R.H., and S.K.W. performed research; M.D. contributed new reagents/analytic tools; H.B.S., R.H., and S.K.W. analyzed data; and H.B.S., R.H., M.D., and E.F.W. wrote the paper.

The authors declare no conflict of interest.

This article is a PNAS Direct Submission.

[1]To whom correspondence should be addressed. E-mail: ewagner@cnio.es.

This article contains supporting information online at www.pnas.org/cgi/content/full/0907550106/DCSupplemental.

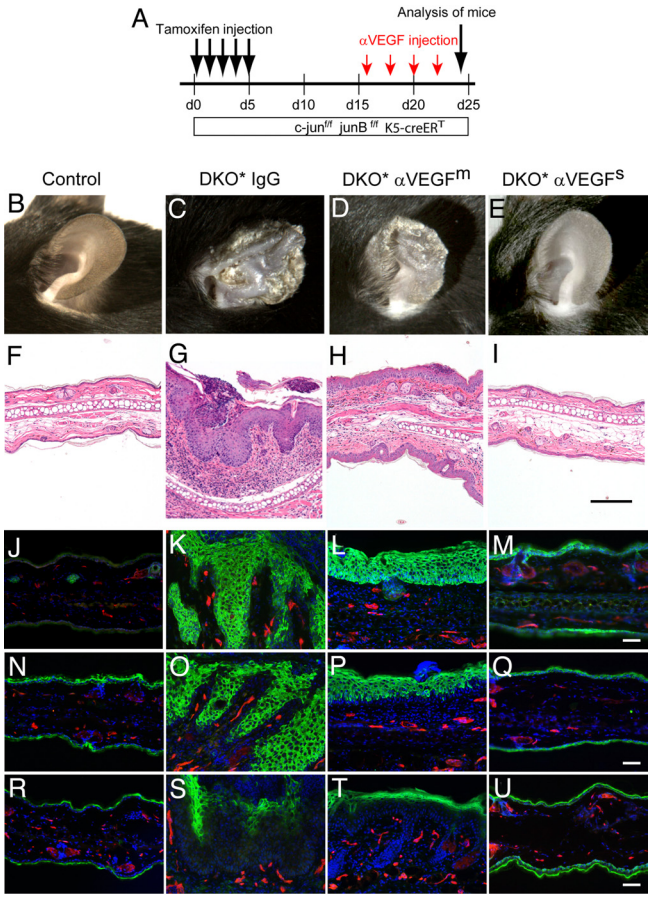

Fig. 1. Systemic inhibition of VEGF alleviates the psoriasis-like phenotype induced by epidermal deletion of *JunB* and *c-Jun*. (*A*) The schematic representation of the experimental procedure. (*B–E*) Ears of control IgG-treated DKO* mice showed prominent inflammatory, scaly skin lesions. Mice that responded only moderately to anti-VEGF antibody treatment (DKO* anti-VEGF^m; $n = 6$) displayed a mild psoriatic phenotype (*D*), whereas the ear skin appeared largely normal in mice with a strong response to the anti-VEGF treatment (DKO* anti-VEGF^s: $n = 5$) (*E*). A control IgG-injected Cre$^-$ mouse is shown for comparison ($n = 3$). (*F–I*) H&E staining of control IgG-treated mice (*F*) and DKO* IgG-treated mice (*G*) reveals the typical signs of the psoriasis-like phenotype. (*H*, *I*) Anti-VEGF–treated mice showed significant improvement in these symptoms. (Scale bars, 100 μm.) (*J–U*) Normalized keratinocyte differentiation after G6–31 treatment. Immunofluorescence analyses showed strong induction of the hyperproliferation marker keratin 6 (*K*) and altered expression patterns of the epidermal differentiation-related proteins keratin 10 (*O*) and loricrin (*S*) in the isotype control IgG-treated DKO* mice, whereas after anti-VEGF treatment the expression patterns normalized showing reduced expression of keratin 6 (*L*, *M*) and restriction of the expression of keratin 10 (*P*, *Q*) and loricrin (*T*, *U*) to the suprabasal layers of the epidermis. A normal control mouse is shown for comparison (*J*, *N*, *R*). Blood vessels (MECA-32$^+$) are shown in red; nuclei are stained in blue (Hoechst 33342 stain). (Scale bars, 50 μm.)

tion), they received 4 consecutive injections of the anti-VEGF antibody or an isotype control IgG every second day (Fig. 1*A*). The appearance of the phenotype was determined by macroscopically visible scaly areas on ears and tail. At day 23–24, the double-knockout (DKO*) mice injected with isotype control IgG ($n = 8$) showed prominent inflammatory, scaly skin lesions on the ears (Fig. 1*C*). The skin of the paws and tails showed the typical signs of psoriasis macroscopically as well as in histological analysis [supporting information (SI) Fig. S1 *A* and *B*]. In contrast, Cre$^-$ mice injected with either isotype control IgG ($n = 3$) or anti-VEGF ($n = 2$) did not show any skin abnormalities (Figs. 1*B* and S1*B*). However, systemic treatment with the anti-VEGF antibody for 8 days resulted in an almost complete reduction of skin inflammation, scaliness, and swelling in 5 of 12 treated mice (referred to as strong responders, "DKO* anti-VEGF^s"; Fig. 1*E*). Six of 12 treated mice showed a moderate anti-inflammatory response in the ears (referred to as moderate responders, "DKO* anti-VEGF^m"; Fig. 1*D*). No major response was observed in only 1 mouse. The differences between strong responders (5 of 12 mice) versus moderate responders (6 of 12 mice) to the anti-VEGF treatment might result from the variability observed in biological systems or might be explained by the complexity of the phenotype and the mixed genetic background. The anti-VEGF treatment of DKO* mice also ameliorated the psoriasis-like symptoms in the paws and in the tails (Fig. S1 *A* and *B*). Dramatically reduced redness and swelling of the toes was observed in anti-VEGF–treated mice (Fig. S1*A*). These findings indicate that inhibition of the angiogenic growth factor VEGF is able to reverse the psoriasis-like skin phenotype including the epidermal abnormalities.

Anti-VEGF Treatment Normalizes the Epidermal Architecture in Inflamed Skin. To characterize better the efficacy of systemic VEGF blockade in reducing psoriasis-like skin inflammation, histological analyses were performed on ear sections obtained from DKO* mice and Cre$^-$ littermate controls treated with anti-VEGF or with isotype control IgG. After 8 days of treatment, H&E-stained sections revealed the typical histopathological signs of the psoriasis-like phenotype in the IgG-treated DKO* mice, i.e., acanthosis (thickened epidermis), hyperkeratosis (thickening of the stratum corneum), parakeratosis (retention of nuclei in the stratum corneum), epidermal rete-ridge projections into the dermis, and microabscesses (Fig. 1*G*). In contrast, systemic inhibition of VEGF led to a noticeable reduction in the psoriasis-like histological features (Fig. 1 *H* and *I*).

The epidermal hyperproliferation marker keratin 6 is normally absent from interfollicular epidermis, whereas keratin 10 is expressed in the suprabasal layers of the normal epidermis. During psoriatic hyperproliferation of keratinocytes, both keratin 6 and keratin 10 display a much broader staining pattern. Treatment with the anti-VEGF antibody for 8 days normalized the expression of both keratin 6 (Fig. 1 *L* and M) and keratin 10 (Fig. 1 *P* and Q) to a staining pattern much more similar to that observed in uninflamed epidermis (Fig. 1 *J* and *N*), unlike the inflamed epidermis of isotype control-treated mice (Fig. 1 *K* and *O*). After anti-VEGF treatment, loricrin, a marker of epidermal cornification, was restricted largely to the upper granular layer (Fig. 1 *T* and *U*), as typically observed in normal epidermis (Fig. 1*R*). By contrast, loricrin expression was increased, was more focal, and was present in several keratinocyte layers in the ears of isotype control-treated mice (Fig. 1*S*). Thus, inhibition of VEGF normalized the epidermal skin architecture in this mouse model of psoriasis.

As reported earlier, deletion of *JunB* and *c-Jun* in the epidermis leads to up-regulation of the chemotactic proteins S100A8 and S100A9 in the epidermis before the onset of disease symptoms (23). To corroborate the observation in DKO* mice, we analyzed sections for up-regulation of the S100A8 and S100A9 proteins (Fig. 2 *B–D* and *F–H*). Both groups, DKO* IgG-treated and DKO* anti-VEGF–treated, displayed the characteristic up-regulation of these 2 proteins in the epidermis. Quantification of S100A8 levels by Western blot showed only a slight reduction of S100A8 protein in the epidermis of anti-VEGF–treated mice compared with DKO* IgG–treated mice (Fig. 2 *S* and *T*). Furthermore, the apparent increase of S100A8$^+$ cells in the dermis of DKO*IgG-treated mice was region specific and was reduced in anti-VEGF–treated mice (Fig. 2 *F–H*).

To investigate the proliferative activity in the skin, the number of Ki67$^+$ proliferating epidermal keratinocytes and dermal cells was measured and was found to be markedly reduced in both moderate and strong anti-VEGF responders (Fig. 2 *K*, *L*, and *Q*), suggesting reduced proliferative activity of keratinocytes after anti-VEGF treatment. Staining for phosphorylation of histone H3 serine 10

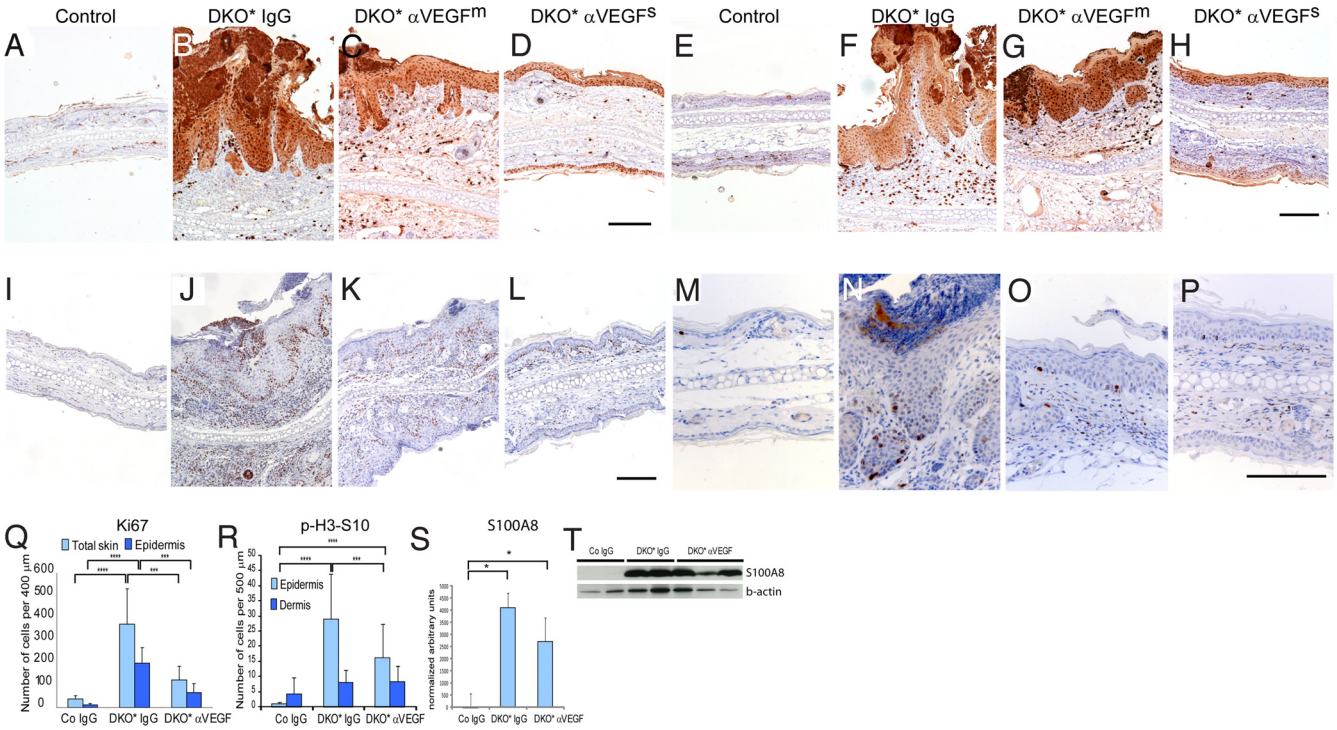

Fig. 2. Induction of downstream targets *S100A8* and *S100A9* but normalized keratinocyte proliferation after G6–31 treatment. Immunohistochemistry of *S100A9* (*A–D*) and *S100A8* (*E–H*), target genes of Jun proteins, showed an up-regulation in both IgG-treated mice (*B*, *F*) and anti-VEGF–treated DKO* mice (*C*, *D*, *G*, *H*) after the deletion of *JunB* and *c-Jun*. (*I–L*) Ki67 staining shows a significant reduction of proliferation in anti-VEGF–treated animals (*K*, *L*, *Q*; total skin: $P < 2.21E\text{-}08$; epidermis only: $P < 0.00022$) compared with DKO* IgG-injected mice (*J*). Moreover, staining for the histone H3 phosphorylation on serine 10 (P-H3-S10) revealed that the proliferation is more pronounced in the epidermis than in the dermis (*M–P*, *R*; epidermis control IgG-treated vs. DKO* IgG-treated: $P < 5.7E\text{-}08$; epidermis DKO* IgG-treated vs. DKO* anti-VEGF–treated: $P < 9.7E\text{-}05$; epidermis control IgG-treated vs. DKO* anti-VEGF–treated: $P < 1.0E\text{-}05$). Data represent mean ± SD. (Scale bars, 100 μm.) Quantification of Western blots of epidermal samples showed similar levels of S100A8 protein in DKO* IgG-treated and anti-VEGF–treated mice (*S* and *T*).

(P-H3-S10) was performed to investigate the proliferation activity in the epidermis and dermis in more detail (Fig. 2 *M–P*). The quantification of cells positive for P-H3-S10 showed that proliferation activity is higher in the epidermis in DKO* IgG-treated mice than in control mice ($P < 0.0001$, Fig. 2*R*), and proliferation in the epidermis is reduced in anti-VEGF–treated mice ($P < 0.001$; Fig. 2*R*) compared with DKO* IgG-treated mice.

Reduced Vascular Abnormalities Following Anti-VEGF Treatment. Differential immunofluorescence analyses of MECA-32$^+$ blood vessels and of CD31$^+$/lymphatic vessel endothelial hyaluronan receptor-1 (LYVE-1)$^+$ lymphatic vessels revealed that the inhibition of VEGF led to a strong decrease in tissue vascularization (Fig. 3 *C*, *D*, *G*, and *H*) compared with control mice (Fig. 3 *B* and *F*). No vascular abnormalities were found in isotype control IgG-treated Cre$^-$ - mice (Fig. 3 *A* and *E*). Computer-assisted image analysis revealed that the average ear thickness ($P < 0.01$; Fig. 3*I*) and epidermal thickness ($P < 0.01$; Fig. 3*J*) were significantly reduced after treatment with the anti-VEGF antibody. Importantly, the average number of blood vessels was significantly reduced ($P < 0.001$; Fig. 3*K*) and the average size of blood vessels ($P < 0.001$; Fig. 3*L*) and lymphatic vessels ($P < 0.001$; Fig. 3*M*) was significantly smaller in G6–31–treated mice than in isotype control-treated animals. The average number of lymphatic vessels was indistinguishable between the 2 groups (Fig. 3*N*). Thus, inhibition of VEGF-dependent pathological angiogenesis normalized the blood and lymphatic vasculature.

Inhibition of VEGF Reduces Leukocyte and Lymphocyte Infiltration in the Skin. To characterize the immune infiltrate in the skin, we analyzed by immunohistochemistry the expression of a neutrophilic cell marker, Gr-1, and myeloid peroxidase (MPO) (Fig. 4 *A–D* and Fig. S1 *D* and *F*) and the expression of the 2 macrophage markers CD11b and F4/80 (Fig. 4 *E–L*). The inflamed skin of isotype control-treated mice contained increased numbers of dermal Gr-1$^+$, CD11b$^+$, and F4/80$^+$ leukocytes (Fig. 4 *B*, *F*, and *J*). In contrast, the overall number of leukocytes in the skin of anti-VEGF–treated mice was reduced compared with isotype control-treated animals (Fig. 4 *C*, *D*, *G*, *H*, *K*, and *L*). Quantitative analyses indicated that the number of MPO$^+$ neutrophils and F4/80$^+$ macrophages was significantly reduced ($P = 0.0068$ and $P = 0.00027$, respectively) (Fig. S1 *F* and *G*). In particular, the number of Gr-1$^+$ neutrophilic granulocytes was greatly reduced, and no transmigration of these cells through the epidermis was seen after anti-VEGF treatment (Fig. 4 *C* and *D*). We performed staining for S100A4, which labels Langerhans cells (26), to investigate in more detail the presence of these cells after anti-VEGF treatment (Fig. S1*C*). The number of S100A4$^+$ cells was reduced in the epidermis of DKO* anti-VEGF–treated mice (Fig. S1*I*). Fibroblasts in the dermis also were positive for S100A4.

Similar to the pathophysiology seen in human psoriatic plaques, the number of dermal CD3$^+$ T lymphocytes was increased in anti-IgG–treated DKO* mice (Fig. 4*N*) compared with their Cre$^-$ littermates (Fig. 4*M*). However, fewer dermal and intraepidermal CD3$^+$ T lymphocytes were detected in sections from anti-VEGF–treated mice (Fig. 4 *O* and *P*). Quantification of these cells showed a significant reduction of CD3$^+$ T lymphocytes in the epidermis as well as in the dermis (epidermis: $P = 0.00108$; total skin: $P = 0.00150$; Fig. S1*H*). The same results were obtained by immunohistochemical staining for CD4$^+$ T lymphocytes (Fig. 4 *S* and *T*). Thus, specific inhibition of VEGF reversed the inflammatory infiltrate typically associated with psoriasis. Finally, as known from human psoriasis, the B-cell compartment assessed by Pax5$^+$ cells (Fig. S1*E*) displayed neither an increase nor a decrease in DKO*

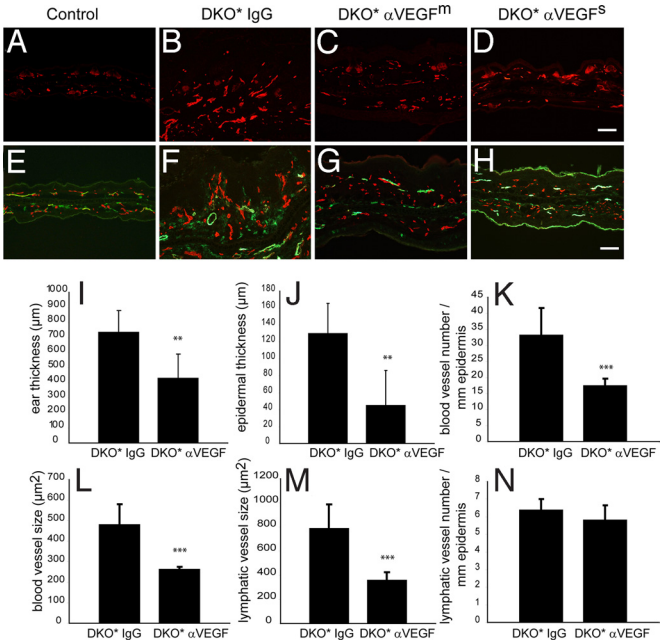

Fig. 3. Reduced vascular abnormalities after G6–31 treatment. (*A–D*) Immunostaining for MECA-32 showed increased vascular density and enlargement of blood vessels in the control IgG-treated group (*B*), compared with anti-VEGF–treated mice (*C, D*) or normal Cre$^-$ control mice (*A*). (*E–H*) Double immunofluorescence staining for CD31 (red) and for LYVE-1 (green) revealed enlarged lymphatic vessels in the skin of isotype control IgG-treated mice (*F*) compared with anti-VEGF–treated mice (*G, H*) or normal control mice (*E*). The positive staining of LYVE-1 in the stratum corneum in *H* is unspecific. (Scale bars, 100 μm.) (*I–N*) Computer-assisted measurements demonstrated that the ear thickness (*I*) and epidermal thickness (*J*) were significantly reduced after anti-VEGF mAb treatment (**, $P < 0.01$), as compared with the control treated group. (*K–N*) The average size of blood (*L*) and lymphatic (*M*) vessels and the number of blood vessels in the skin (*K*) were significantly reduced after systemic inhibition of VEGF (***, $P < 0.001$). No significant difference in the number of lymphatic vessels was found in the 2 groups (*N*). Data represent mean ± SD.

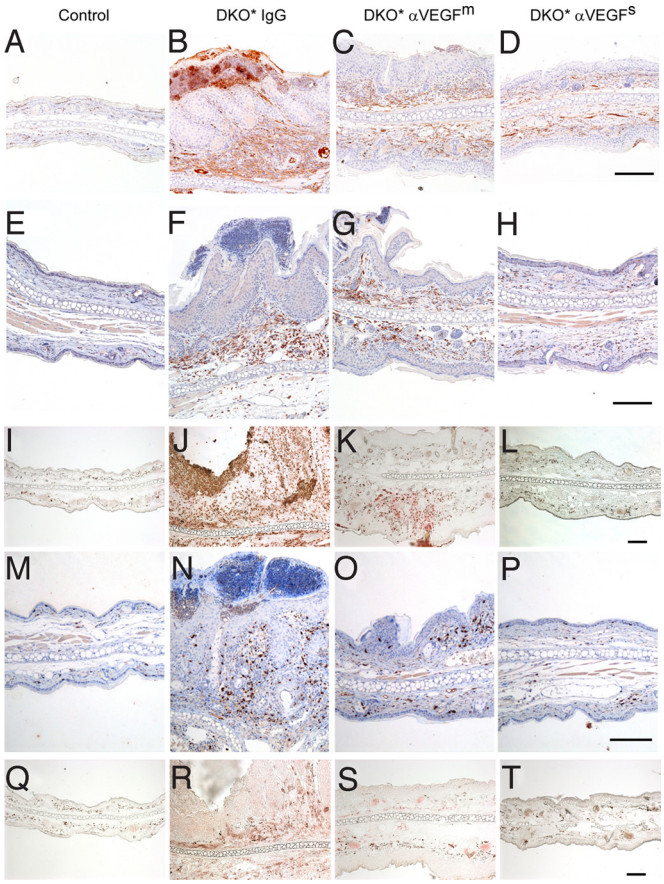

Fig. 4. Inhibition of VEGF reduces macrophage and lymphocyte infiltration. Immunohistochemistry for leukocyte markers Gr-1 (*A–D*), F4/80 (*E–H*), and CD11b (*I–L*) revealed decreased dermal leukocyte infiltration (*C, D, G, H, K, L*) and decreased epidermal as well as dermal CD3$^+$ and CD4$^+$ T lymphocytes (*O, P, S, T*) in the skin of anti-VEGF–treated mice, as compared with the IgG-treated group (*B, F, J, N, R*). A normal Cre$^-$ control mouse is shown for comparison (*A, E, I, M, Q*). (Scale bars, 100 μm in *A–H* and *M–P* and 50 μm in *I–P* and *Q–T*.)

mice treated with IgG or anti-VEGF compared with controls. We cannot formally exclude an immune reaction caused by the injection of the humanized forms of IgG and anti-VEGF. However, increased inflammation was not detected in the control mice injected with either IgG ($n = 3$) or anti-VEGF ($n = 2$).

Molecular Analyses of Anti-VEGF Treated Mice. We next performed RT-PCR analyses in separated epidermis of anti-VEGF–treated mice for selected *Jun* target genes as well as for markers of angiogenesis, inflammation, and epidermal differentiation. RNA levels, which were elevated for *VEGF* in the DKO*IgG-treated mice, were significantly reduced in anti-VEGF–treated mice (Fig. 5*A*). The same results were obtained for the expression levels for *VEGFR1* and *VEGFR2* (Fig. 5 *B* and *C*). Similar results for *VEGF*, *VEGFR1*, and *VEGFR2* also have been observed previously in human psoriatic skin samples (27, 28). Even though protein levels of S100A8 and S100A9 in the antibody staining and the Western blots remained similar, the RNA levels for *S100A8* and *S100A9* were reduced significantly in epidermal samples of anti-VEGF–treated mice (Fig. 5 *D* and *E*). Interestingly, expression levels for *S100A7A*, the closest mouse homologue to human psoriasin, were also significantly reduced (Fig. 5*F*). Furthermore, *MIP-1α* and *MIP-1β*, chemokines providing a strong T-cell chemotactic effect, were found to be highly expressed in the epidermis of IgG-treated DKO* mice (Fig. S2 *A* and *B*). *Macrophage inflammatory protein-2* (*MIP-2*; *IL-8* in humans), a strong chemoattractant for neutrophils and T cells produced mainly by keratinocytes, also was found to be strongly expressed in DKO* IgG-treated mice but was reduced to control levels in anti-VEGF–treated mice (Fig. S2*C*), in agreement with the anti-inflammatory effect of anti-VEGF treatment. RT-PCR analysis of *IL-1β* and chemokine (C-X-C motif) ligand 2 (*CXCL2*) from total skin also showed normalization in expression levels (Fig. 5 *G* and *H*). Moreover, a significant decrease of serum levels for regulated upon activation, normal HYPERLINK "http://www.copewithcytokines.de/cope.cgi?key=T%2dcells" T-cell expressed, and presumably secreted (*RANTES*) but only slightly decreased levels for monocyte chemotactic protein 1 (*MCP-1*) were observed (Fig. S2 *D* and *E*).

The normalization of epidermal differentiation detected in the histological analysis was confirmed by RT-PCR analysis, because mRNA levels of *keratins 1* (*K1*), *5* (*K5*), and *14* (*K14*) were found to be reduced (Fig. S2 *F–H*). Moreover, levels for *keratin 15* (*K15*), known to be down-regulated in psoriatic lesions, reverted to control levels in anti-VEGF–treated mice (Fig. S2*I*).

Isotype control-treated DKO* mice showed a strong increase in expression of *matrix metalloproteinase 3* (*MMP3*), *MMP8*, and *MMP9*, markers of inflammation and tissue repair. In contrast, the expression levels of these genes were markedly reduced in anti-VEGF–treated mice (Fig. 5 *I* and *J* and Fig. S2*J*), indicating an overall reduced inflammation in anti-VEGF–treated mice. This observation is supported by the normalization of RNA levels of *MMP2* and *IL-6* (Fig. 5*K* and Fig. S2*K*). In contrast, tissue inhibitor of metalloproteinases-3 (*TIMP3*) levels remained down-regulated

IMMUNOLOGY

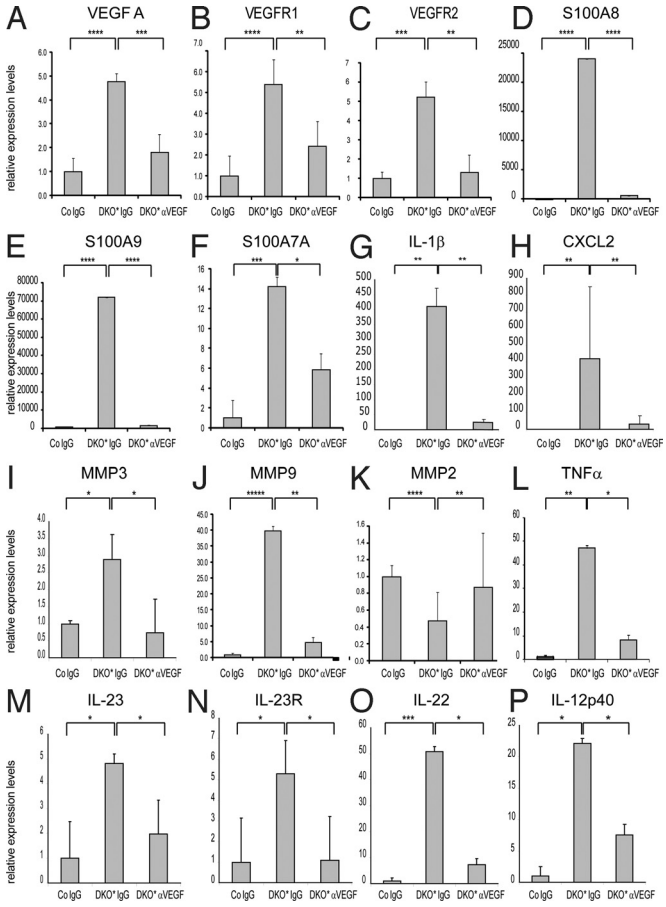

Fig. 5. Expression analyses of genes involved in inflammation and epidermal differentiation. RT-PCR analysis of mRNA expression levels revealed strong expression of *VEGF A*, VEGFR1, and VEGFR2 in DKO* IgG-treated mice which was reduced in DKO* anti-VEGF–treated mice (*A–C*). *S100A8* (*D*) and *A9* (*E*) were increased in DKO* mice and decreased in anti-VEGF–injected mice, perhaps because of a posttranslational mechanism or a negative feedback loop. The expression levels of epidermal samples of the following genes (especially cytokines related to the IL-23/Th17 axis and the related receptors) reflect a normalization of the inflammatory process in anti-VEGF–injected mice: *S100A7A* (*F*), *MMP3* (*I*), *MMP9* (*J*), *MMP2* (*K*), *TNFα* (*L*), *IL-23* (*M*), *IL-23R* (*N*), *IL-22* (*O*), and *IL-12p40* (*P*). RNA expression levels of total skin for *IL-1β* (*G*) and *CXCL2* (*H*) also are reduced back to control levels in anti-VEGF–injected mice. Controls are set to 1, and the *y* axis shows relative expression levels. Control IgG-treated: $n = 3$; DKO* IgG-treated: $n = 3–4$; DKO* anti-VEGF–treated: $n = 4–5$. *D–F* represent data (mean ± SD) from control IgG-treated: $n = 3$; DKO* IgG-treated: $n = 5–6$; DKO* anti-VEGF–treated: $n = 10–12$.

in DKO* anti-VEGF–treated mice (Fig. S2*L*), as expected because of the deletion of *c-Jun* and *JunB*. Most importantly, RNA levels of cytokines such as *TNFα* and *IL-23*, known from human data to be highly important in the pathophysiology of psoriasis (29), were significantly reduced in anti-VEGF–treated mice but were strongly increased in DKO* anti-IgG–treated mice. Notably, *TNFα*, *IL-23*, *IL-23R*, *IL-22*, and *IL-12p40* were reduced to normal levels after anti-VEGF treatment (Fig. 5 *L–P*). Therefore, anti-VEGF treatment of mutant mice led to the normalization of the IL-23/T-helper-17 (Th17) axis and consequently to an amelioration of the phenotype.

Discussion

Psoriasis is a common inflammatory skin disease that is heterogeneous, and its pathogenesis still is not well understood. Importantly, therapeutic interventions currently are limited and are restricted to the treatment of symptoms rather than targeting the mechanisms underlying the disease. Our study, employing a therapeutical design, reveals that systemic administration of an anti-VEGF antibody effectively inhibited pathological angiogenesis. Characteristic psoriasis-like symptoms observed in the skin lesions of these mice, such as epidermal hyperplasia with altered differentiation, inflammatory cell infiltration, vascular abnormalities, and elevated levels of IL-23/Th17-related cytokines, were markedly reduced following treatment with anti-VEGF antibody.

In cutaneous lesions and in the serum of psoriatic patients, elevated levels of IL-23 and Th17-related cytokines were detected, and the development and maintenance of Th17 cells has been shown to be linked to IL-23, a key cytokine in the development of autoimmunity (30, 31). Injection of IL-23 in mice leads to erythema, mixed dermal infiltrate, and epidermal hyperplasia associated with parakeratosis comprising histopathological features resembling psoriasis. These responses were shown to be mediated by TNFα and IL-20R2 (32). Moreover, variants of the *IL-23R* gene are associated with psoriasis (33), demonstrating the relevance of IL-23/IL-23R signaling in psoriasis. The common subunit IL-12/IL-23, IL12p40, and IL-23p19 were highly expressed in psoriatic skin lesions as compared with uninvolved skin (34). Moreover, ectopic expression of *IL12p40* from the keratin 14 promoter led to enhanced expression of *IL-23p19* in mouse keratinocytes (35).

A strong increase of TNFα is observed following deletion of *JunB* and *c-Jun* in epidermal tissues during pre- and postnatal development (Fig. 5*L* and refs. 23 and 36). Because TNFα can regulate IL-6 as well as MMP9 levels (37–39), the increase in TNFα could be responsible for the increased VEGF levels in the DKO* mice. In mice, the embryonic fibroblasts *JunB* and *c-Jun* are required for hypoglycemia-induced expression of VEGF (40). However, we favor the hypothesis that induction of VEGF in keratinocytes is mediated instead by a cytokine-dependant mechanism.

Besides cytokines, chemoattractant molecules such as S100A8 and S100A9 are increased in DKO* mice at the protein level (Fig. 2 *B*, *F*, *S*, and *T*). Interestingly, RNA levels of *S100A8* and *S100A9* appear to be decreased in anti-VEGF–treated DKO* mice (Fig. 5 *D* and *E*); this reduction might be caused by a posttranslational mechanism or by an unknown negative feedback loop.

Our findings strongly indicate that therapeutic intervention at the level of the vasculature can be sufficient to reduce the immune-mediated and epidermal components of the disease. We speculate that the anti-inflammatory effects of anti-VEGF antibody treatment block VEGF effects in endothelial cells and also in other cell types in the skin. Besides its role in angiogenesis, VEGF is a well-documented regulator of various aspects of the inflammatory response, wound healing, and tumor growth (41). VEGF induces hyperpermeability of blood vessels, leading to tissue edema during inflammation (42). Furthermore, chronic overexpression of VEGF in the skin of K14-VEGF transgenic mice promoted leukocyte rolling and adhesion in skin microvessels, probably resulting from the increased expression of adhesion molecules such as E- and P-selectin (43). In addition to endothelial cells, monocytes and macrophages also express *VEGFR-1*, and VEGF can chemoattract these cells (44). Thus, the inhibition of these additional activities of VEGF related to attracting and activating immune cells by systemic treatment with an anti-VEGF antibody probably contributed to the diminished inflammatory cell infiltration observed in the skin.

Recent evidence indicates that, lymphangiogenesis, as well as angiogenesis, is involved in certain inflammatory and autoimmune conditions. It is proposed that lymphatic vessel formation and remodeling participates in the regulation of the immune response by affecting the transport of antigens and leukocytes to draining lymph nodes (45). It was recently shown that VEGF can promote lymphangiogenesis associated with tumor formation, tissue repair, and inflammation (7, 46, 47). However, the exact role of lymphatic vessels in inflammation remains to be established.

Whether anti-angiogenic therapy for benign diseases such as psoriasis or rheumatoid arthritis is a viable option will require

additional experiments in other model systems. Moreover, topical application might provide a valuable alternative to overcome unwanted side effects. Nevertheless, these findings provide a proof of concept for the proposition that inflammatory diseases can be treated by anti-angiogenic therapies.

Materials and Methods

Mouse Strains and Treatment. Mice carrying *JunB* and *c-Jun* alleles flanked by loxP sites and the K5-CreER^T allele were used in this study (23). DKO* mice were injected i.p. with 1 mg tamoxifen (Sigma) for 5 consecutive days to induce the deletion of the 2 genes in the epidermis. Mice showing the first signs of the psoriasis-like phenotype were injected every 48 h with 4 doses of the monoclonal antibody G6–31 (25) or a human control IgG. All mouse experiments were performed in accordance with local and institutional regulations and licenses.

Immunohistochemistry and Immunofluorescence. Mice were killed, and ears were collected and cut in half. One half of each ear was processed for paraffin sections. The other half was embedded in optimal cutting temperature (OCT) compound, and 7-μm cryostat sections were cut. Immunohistological analyses were performed as described previously (7, 48).

For paraffin embedding, tissues were fixed in 3.7% paraformaldehyde in PBS at 4 °C overnight. For H&E staining, 3-μm sections of formalin-fixed samples were processed according to standard procedures. Staining for MPO (Dako) and immunohistochemistry with antibodies against CD3 (Vector Laboratories), S100A8, and S100A9 (both Santa Cruz) was performed as described previously (23, 49, 50) or according to the manufacturer's protocol.

Additional Information. For information on computer-assisted morphometric analyses, statistical analysis, and quantitative RT-PCR, see *SI Materials and Methods*.

ACKNOWLEDGMENTS. We thank Maria Helena Idarraga-Amado, Jessica Rubio, and Jeannette Scholl for their excellent technical support and Drs. Latifa Bakiri, Aline Bozec, Juan Guinea Viniegra, Mirna Pérez-Moreno, Maria Sibilia, and Erwin Tschachler for discussions and for critically reading the manuscript. This work was supported by National Institutes of Health Grant CA69184, Swiss National Fund Grant 3100A0–108207, Austrian Science Foundation Grant NFN S94-SP11, the Commission of the European Communities Grant LSHC-CT-2005–518178 (to M.D.) and the Banco Bilbao Vizcaya Argentaria (BBVA)-Foundation. The Research Institute of Molecular Pathology is supported by Boehringer Ingelheim Inc.

1. Carmeliet P (2003) Angiogenesis in health and disease. *Nat Med* 9(6):653–660.
2. Pober JS, Sessa WC (2007) Evolving functions of endothelial cells in inflammation. *Nature Reviews Immunology* 7(10):803–815.
3. Leong TT, Fearon U, Veale DJ (2005) Angiogenesis in psoriasis and psoriatic arthritis: Clues to disease pathogenesis. *Current Rheumatology Reports* 7(4):325–329.
4. Danese S, et al. (2006) Angiogenesis as a novel component of inflammatory bowel disease pathogenesis. *Gastroenterology* 130(7):2060–2073.
5. Bainbridge J, Sivakumar B, Paleolog E (2006) Angiogenesis as a therapeutic target in arthritis: Lessons from oncology. *Current Pharmaceutical Design* 12(21):2631–2644.
6. Xia YP, et al. (2003) Transgenic delivery of VEGF to mouse skin leads to an inflammatory condition resembling human psoriasis. *Blood* 102(1):161–168.
7. Kunstfeld R, et al. (2004) Induction of cutaneous delayed-type hypersensitivity reactions in VEGF-A transgenic mice results in chronic skin inflammation associated with persistent lymphatic hyperplasia. *Blood* 104(4):1048–1057.
8. Detmar M, et al. (1994) Overexpression of vascular permeability factor/vascular endothelial growth factor and its receptors in psoriasis. *J Exp Med* 180(3):1141–1146.
9. Nielsen HJ, et al. (2002) Elevated plasma levels of vascular endothelial growth factor and plasminogen activator inhibitor-1 decrease during improvement of psoriasis. *Inflammation Research* 51(11):563–567.
10. Young HS, Summers AM, Bhushan M, Brenchley PE, Griffiths CE (2004) Single-nucleotide polymorphisms of vascular endothelial growth factor in psoriasis of early onset. *J Invest Dermatol* 122(1):209–215.
11. Halin C, et al. (2008) Inhibition of chronic and acute skin inflammation by treatment with a vascular endothelial growth factor receptor tyrosine kinase inhibitor. *Am J Pathol* 173(1):265–277.
12. Krueger GG, et al. (2007) A human interleukin-12/23 monoclonal antibody for the treatment of psoriasis. *N Engl J Med* 356(6):580–592.
13. Ding C, Xu J, Li J (2008) ABT-874, a fully human monoclonal anti-IL-12/IL-23 antibody for the potential treatment of autoimmune diseases. *Current Opinion in Investigational Drugs* 9(5):515–522.
14. Leonardi CL, et al. (2008) Efficacy and safety of ustekinumab, a human interleukin-12/23 monoclonal antibody, in patients with psoriasis: 76-week results from a randomised, double-blind, placebo-controlled trial (PHOENIX 1). *Lancet* 371(9625):1665–1674.
15. Menter A, Griffiths CE (2007) Current and future management of psoriasis. *Lancet* 370(9583):272–284.
16. Halverstam CP, Lebwohl M (2008) Nonstandard and off-label therapies for psoriasis. *Clinics in Dermatology* 26(5):546–553.
17. Kerr DJ (2004) Targeting angiogenesis in cancer: Clinical development of bevacizumab. *Nature Clinical Practice Oncology* 1(1):39–43.
18. Folkman J (2006) Angiogenesis. *Annu Rev Med* 57 S1–18.
19. Akman A, Yilmaz E, Mutlu H, Ozdogan M (2008) Complete remission of psoriasis following bevacizumab therapy for colon cancer. *Clin Exp Dermatol.* 34(5):e202–204.
20. Zenz R, Wagner EF (2006) Jun signalling in the epidermis: From developmental defects to psoriasis and skin tumors. *Int J Biochem Cell Biol* 38(7):1043–1049.
21. Zenz R, et al. (2003) c-Jun regulates eyelid closure and skin tumor development through EGFR signaling. *Dev Cell* 4(6):879–889.
22. Meixner A, et al. (2008) Epidermal JunB represses G-CSF transcription and affects haematopoiesis and bone formation. *Nat Cell Biol* 10(8):1003–1011.
23. Zenz R, et al. (2005) Psoriasis-like skin disease and arthritis caused by inducible epidermal deletion of Jun proteins. *Nature* 437(7057):369–375.
24. Zenz R, et al. (2008) Activator protein 1 (Fos/Jun) functions in inflammatory bone and skin disease. *Arthritis Research and Therapy*10(1):201.
25. Liang WC, et al. (2006) Cross-species vascular endothelial growth factor (VEGF)-blocking antibodies completely inhibit the growth of human tumor xenografts and measure the contribution of stromal VEGF. *J Biol Chem* 281(2):951–961.
26. Zibert JR, Skov L, Thyssen JP, Jacobsen GK, Grigorian M (July 30, 2009) Significance of the S100A4 protein in psoriasis. *J Invest Dermatol*, 10.1038/jid.2009.206.
27. Man XY, Yang XH, Cai SQ, Yao YG, Zheng M (2006) Immunolocalization and expression of vascular endothelial growth factor receptors (VEGFRs) and neuropilins (NRPs) on keratinocytes in human epidermis. *Molecular Medicine* 12(7–8):127–136.
28. Man XY, Yang XH, Cai SQ, Bu ZY, Zheng M (2008) Overexpression of vascular endothelial growth factor (VEGF) receptors on keratinocytes in psoriasis: Regulated by calcium independent of VEGF. *Journal of Cellular and Molecular Medicine* 12(2):649–660.
29. Di Cesare A, Di Meglio P, Nestle FO (2009) The IL-23/Th17 axis in the immunopathogenesis of psoriasis. *J Invest Dermatol* 129(6):1339–1350.
30. Bettelli E, et al. (2006) Reciprocal developmental pathways for the generation of pathogenic effector TH17 and regulatory T cells. *Nature* 441(7090):235–238.
31. Kastelein RA, Hunter CA, Cua DJ (2007) Discovery and biology of IL-23 and IL-27: Related but functionally distinct regulators of inflammation. *Annu Rev Immunol* 25:221–242.
32. Chan JR, et al. (2006) IL-23 stimulates epidermal hyperplasia via TNF and IL-20R2-dependent mechanisms with implications for psoriasis pathogenesis. *J Exp Med* 203(12):2577–2587.
33. Nair RP, et al. (2008) Polymorphisms of the IL12B and IL23R genes are associated with psoriasis. *J Invest Dermatol* 128(7):1653–1661.
34. Lee E, et al. (2004) Increased expression of interleukin 23 p19 and p40 in lesional skin of patients with psoriasis vulgaris. *J Exp Med* 199(1):125–130.
35. Kopp T, et al. (2003) IL-23 production by cosecretion of endogenous p19 and transgenic p40 in keratin 14/p40 transgenic mice: Evidence for enhanced cutaneous immunity. *J Immunol* 170(11):5438–5444.
36. Guinea-Viniegra J, et al. (2009) TNFalpha shedding and epidermal inflammation are controlled by Jun proteins. *Genes Dev* 23:2663–2674.
37. Scott KA, et al. (2004) TNF-alpha regulates epithelial expression of MMP-9 and integrin alphavbeta6 during tumour promotion. A role for TNF-alpha in keratinocyte migration? *Oncogene* 23(41):6954–6966.
38. Rega G, et al. (2007) Vascular endothelial growth factor is induced by the inflammatory cytokines interleukin-6 and oncostatin m in human adipose tissue in vitro and in murine adipose tissue in vivo. *Arterioscler Thromb Vasc Biol* 27(7):1587–1595.
39. Bergers G, et al. (2000) Matrix metalloproteinase-9 triggers the angiogenic switch during carcinogenesis. *Nat Cell Biol* 2(10):737–744.
40. Textor B, Sator-Schmitt M, Richter KH, Angel P, Schorpp-Kistner M (2006) c-Jun and JunB are essential for hypoglycemia-mediated VEGF induction. *Ann N Y Acad Sci* 1091:310–318.
41. Rossiter H, et al. (2004) Loss of vascular endothelial growth factor a activity in murine epidermal keratinocytes delays wound healing and inhibits tumor formation. *Cancer Res* 64(10):3508–3516.
42. Ferrara N, Gerber HP, LeCouter J (2003) The biology of VEGF and its receptors. *Nat Med* 9(6):669–676.
43. Detmar M, et al. (1998) Increased microvascular density and enhanced leukocyte rolling and adhesion in the skin of VEGF transgenic mice. *J Invest Dermatol* 111(1):1–6.
44. Sawano A, et al. (2001) Flt-1, vascular endothelial growth factor receptor 1, is a novel cell surface marker for the lineage of monocyte-macrophages in humans. *Blood* 97(3):785–791.
45. Angeli V, et al. (2006) B cell-driven lymphangiogenesis in inflamed lymph nodes enhances dendritic cell mobilization. *Immunity* 24(2):203–215.
46. Hirakawa S, et al. (2005) VEGF-A induces tumor and sentinel lymph node lymphangiogenesis and promotes lymphatic metastasis. *J Exp Med* 201(7):1089–1099.
47. Hong YK, et al. (2004) VEGF-A promotes tissue repair-associated lymphatic vessel formation via VEGFR-2 and the alpha1beta1 and alpha2beta1 integrins. *FASEB J* 18(10):1111–1113.
48. Traxler P, et al. (2004) AEE788: A dual family epidermal growth factor receptor/ErbB2 and vascular endothelial growth factor receptor tyrosine kinase inhibitor with antitumor and antiangiogenic activity. *Cancer Res* 64(14):4931–4941.
49. Gebhardt C, et al. (2008) RAGE signaling sustains inflammation and promotes tumor development. *J Exp Med* 205(2):275–285.
50. Hui L, Zatloukal K, Scheuch H, Stepniak E, Wagner EF (2008) Proliferation of human HCC cells and chemically induced mouse liver cancers requires JNK1-dependent p21 downregulation. *J Clin Invest* 118(12):3943–3953.